

Measurement of electron-impact excitation cross sections out of the neon 3P_2 metastable levelJohn B. Boffard, M. L. Keeler,* Garrett A. Piech,[†] L. W. Anderson, and Chun C. Lin*Department of Physics, University of Wisconsin, Madison, Wisconsin 53706*

(Received 16 April 2001; published 13 August 2001)

We have measured cross sections for the electron-impact excitation out of the metastable levels of neon into the ten levels of the $2p^53p$ configuration. Two sources of metastable neon atoms were used, a hollow-cathode discharge and a fast beam formed via near-resonant charge exchange. Both sources produce a mixed target of Ne in both (3P_0 and 3P_2) metastable levels. For the $2p^53p$ excited levels with $J=2$ or $J=3$, the excitation is dominated by excitation from the 3P_2 level, and we present cross sections over the energy range of 0 to 450 eV. The results are compared with the cross sections for excitation out of the metastable levels of argon and the applications to diagnostics of ionized gas systems are discussed.

DOI: 10.1103/PhysRevA.64.032708

PACS number(s): 34.80.Dp

I. INTRODUCTION

Electron-impact excitation of atoms has been long studied not only for the theoretical insight gained into this fundamental physical process, but also for the many practical applications for cross-section data. Most previous works have concentrated on excitation out of the ground state of atoms. In many applications however, metastable atoms play an important role as intermediaries between the ground level and the final state whether it be an excited atom or ion [1,2]. Examples include plasma processing [3,4], lighting [5], and gas-discharge lasers [2,6]. Comparison of excitation into higher levels from both the ground state and any metastable levels into a common upper level poses an interesting challenge to theoretical calculations. Our measurements of electron-impact excitation out of the metastable levels of neon thus serve as a counterpoint of our group's previous measurements of excitation out of the ground state of neon.

A simplified energy-level diagram for the lowest-lying energy levels of neon is shown in Fig. 1. The ground state of neon is the closed shell $1s^22s^22p^6$. The first set of four excited levels arise from the $2p^53s$ configuration and are labeled $1s_2$ to $1s_5$ in Paschen's notation. The two levels with $J=1$ of this configuration, the $1s_2$ and $1s_4$ levels, are resonant levels with lifetimes (in the absence of radiation trapping) on the order of 2 ns and 20 ns, respectively [7]. The remaining two levels, the $1s_3$ (3P_0) and $1s_5$ (3P_2), are both metastable with lifetimes in excess of 0.8 s [8]. The next set of ten excited levels arise from the $2p^53p$ configuration and are labeled as $2p_1$ through $2p_{10}$ in Paschen's notation with total angular momentum values between $J=0$ and $J=3$ as indicated in Table I.

Cross-section measurements out of the $2p^6$ ground level of neon has been extensively studied for excitation into the levels of the $2p^53s$ configuration [9–11], the $2p^53p$ configuration [10,12–14], and higher levels [12,13]. In contrast, much more limited results have been published for excitation [15–20] and ionization [21,22] out of the metastable levels. In this paper, we present our measurements for excitation out

of the $1s_5$ ($J=2$) metastable level into four levels of the $2p^53p$ configuration over the energy range of 0 to 450 eV. We also report limited results for excitation from a mixed target into the remaining six levels of the $2p^53p$ configuration.

II. METHOD

A. Apparatus

We use the optical method to measure electron-impact excitation cross sections [23]. A monoenergetic electron beam is passed through a metastable atom target. The resulting fluorescence from the decay of atoms excited to higher-lying levels is proportional to the apparent cross section. Two different sources of metastable atoms were used in this paper. For work at low-electron energies (<16 eV), a hollow cathode discharge was used as the source of metastable atoms. For measurements at higher-electron energies (16 eV to 450 eV), a fast beam of metastable atoms formed via near-resonant charge-exchange was used. Both experiments have been described previously [24–27], so only a brief description of each is presented.

1. Hollow-cathode discharge

This apparatus uses a hollow-cathode discharge as a source of metastable atoms. A hole in the base of the dis-

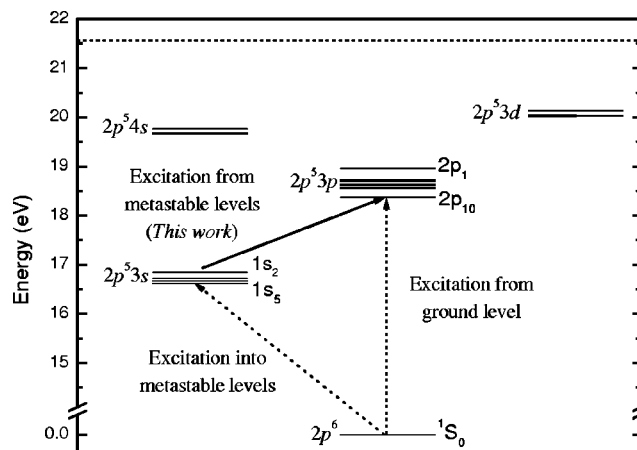


FIG. 1. Simplified Ne energy level diagram.

*Present address: Department of Physics, University of Wisconsin–Superior, Superior, WI.

[†]Present address: Corning Inc. Corning, NY.

TABLE I. Relevant energy levels.

Paschen	Racah	J	Transition Obs.	Wavelength (nm)
$2p_1$	$3p'[1/2]_0$	0	$2p_1 \rightarrow 1s_2$	585.2
$2p_2$	$3p'[1/2]_1$	1	$2p_2 \rightarrow 1s_2$	659.8
$2p_3$	$3p[1/2]_0$	0	$2p_3 \rightarrow 1s_4$	607.4
$2p_4$	$3p'[3/2]_2$	2	$2p_4 \rightarrow 1s_2$	667.8
$2p_5$	$3p'[3/2]_1$	1	$2p_5 \rightarrow 1s_3$	626.6
$2p_6$	$3p[3/2]_2$	2	$2p_6 \rightarrow 1s_2$	692.9
$2p_7$	$3p[3/2]_1$	1	$2p_7 \rightarrow 1s_4$	638.3
$2p_8$	$3p[5/2]_2$	2	$2p_8 \rightarrow 1s_4$	650.7
$2p_9$	$3p[5/2]_3$	3	$2p_9 \rightarrow 1s_5$	640.2
$2p_{10}$	$3p[1/2]_1$	1	$2p_{10} \rightarrow 1s_5$	703.2

charge permit atoms to flow out of the discharge into the collision region. The electron beam crosses the uncollimated atomic beam at right angles. The electron gun used with this experiment typically produces a beam current of $\sim 10 \mu\text{A}$ at 10 eV, with an energy spread less than 0.5 eV. The optical emissions from the decay of excited levels is detected by a photomultiplier (PMT) operating in photon-counting mode. Narrow-band (0.3-1.0 nm) interference filters were used to provide spectral isolation for each transition. The optical system is oriented right angles to the atomic beam and at an angle of 60° to the electron-beam axis.

Only a very small fraction ($\sim 3 \times 10^{-6}$) of the atoms emerging from the discharge are in either of the metastable levels. The remaining large fraction of ground-state atoms limits this apparatus to electron energies below the onset for excitation out of the ground state (~ 18 eV). The metastable target density for this source is approximately $2 \times 10^8 \text{ cm}^{-3}$, with an estimated 5:1 statistical weighting for the ratio of atoms in the $1s_5:1s_3$ metastable levels.

2. Fast beam

The second apparatus we have used in this paper uses near-resonant charge exchange between a fast neon ion beam and a cesium vapor target to produce metastable Ne atoms. Neon ions are extracted from a radio-frequency ion source and accelerated to an energy of 1.6 keV. The focused ion beam is then passed through a recirculating cesium vapor target that converts some of the ions into neutral atoms.

We determine the fraction of $1s_5$ ($J=2$) metastable atoms in the resulting neutral beam as follows. The four levels of the neon $2p^53s$ configuration are near resonant with the ground state of cesium (ΔE between +0.8 eV and +1.1 eV for the four levels). There are no published measurements of the beam composition for charge transfer between 1.6 keV neon ions and cesium. However, measurements of charge transfer between neon and sodium [28,29] as well as between other heavy rare-gas atoms and alkali atoms generally indicate that at low-keV energies, the four levels of the neon $2p^53s$ configuration are populated approximately according to their statistical weights. Following the ground-state decay of the $J=1$ levels, this yields a $^1S_0: ^3P_2: ^3P_0$ beam composition ratio of 6:5:1. The ground-state fraction in our fast beam is slightly higher due to a combination of

resonant charge exchange with background neon gas atoms, and a small correction for the large acceptance angle for our collision region ($\sim 0.25^\circ$) which allows for a small number of nonresonant (large-angle) scattering events that can still enter our collision region. A small amount of resonant charge transfer into the levels of the $2p^53p$ configuration is also possible; however, the measurements of Meyer and Anderson [30] indicate that this is unlikely for beam energies below 10 keV. We thus estimate the fraction of $1s_5$ metastable atoms in our fast beam to be 0.39 ± 0.05 .

After passage through the charge-exchange cell, the remaining ions are removed from the beam by electrostatic deflection plates. The fast neutral beam is then crossed at right angles with an electron beam, and the resulting fluorescence is detected at right angles to both beams. The light is collected by a lens, passed through a narrow-band interference filter, and imaged onto a cooled-PMT operating in photon-counting mode. Typical electron-beam currents for this apparatus were $\sim 150 \mu\text{A}$ at 50 eV, with a ≤ 1 eV energy spread. The atomic beam flux was measured with a combination secondary-electron emission/pyroelectric-film thermal detector [31]. The thermal detector is calibrated by using a fast neon ion beam whose current is also recorded by the neutral detector operating as a Faraday cup. The typical metastable number density using the fast beam source is $\sim 1 \times 10^6 \text{ cm}^{-3}$.

B. Data collection

Final cross-section results were obtained in three steps. First, relative excitation functions (Q vs. E) are obtained for each excited level. This consists of dividing the difference in photon counts with electron beam on/off, by the electron current and neutral beam flux (in the case of the fast beam source, the neutral beam was also modulated by gating the ion beam on/off before it entered the charge-exchange cell). In the second step, the absolute value of the $1s_5 \rightarrow 2p_9$ excitation cross section is found at an energy of 75 eV using the procedure outlined in Sec. II B 1. In the third step, the values of the other $2p^53p$ levels are placed on an absolute scale by ratioing the relative results to the measured $1s_5 \rightarrow 2p_9$ excitation cross section at 10 eV. The details of this procedure are outlined in the Sec. II B 2.

1. Calibration of $2p_9$ level

The absolute calibration procedure, done using the fast beam target, is essentially the same as that used for the absolute calibration of both our previous results with metastable helium and argon fast beam targets. The signal S is recorded for an experiment with a fast metastable beam target (m), and for a static ground-state target (g) obtained by filling the collision chamber with neon gas. The metastable cross section can be found in terms of the known excitation cross section out of the ground state using,

$$Q_m(E) = Q_g(E)(S_m/S_g)C_{\text{overlap}}(E), \quad (1)$$

where C_{overlap} is related to the different beam overlaps for the fast (metastable) beam and the static (ground state) gas targets. In particular,

$$C_{\text{overlap}}(E) = \frac{\int \Phi_s(\vec{r}) n_g(\vec{r}) J(E, \vec{r}) d\vec{r}}{\int \Phi_f(\vec{r}) n_m(\vec{r}) J(E, \vec{r}) d\vec{r}}, \quad (2)$$

where n_m and n_g are the number densities of the metastable and ground-state targets, $J(E)$ is the electron-beam current density, E is the electron energy, and Φ is the probability of detecting a photon from atom excited at position \vec{r} and is qualitatively different for a static gas target (Φ_s) and a fast beam target (Φ_f). More information on the procedures employed to measure the various profiles of the optical system, and the electron and neutral beams can be found in Ref. [32].

The ground-state portion of the experiment is performed with a neon gas pressure of 1.3×10^{-7} Torr (measured by a spinning rotor gauge). We have used the ground state apparent cross sections of Chilton *et al.* [12] extrapolated to zero pressure. At 100 eV, this extrapolation yields a value of the $2p_9$ apparent cross section of $(25 \pm 4) \times 10^{-20}$ cm². This is in excellent agreement with the recent value of $(24.0 \pm 3.4) \times 10^{-20}$ cm² measured by Tsurubuchi *et al.* [10].

The uncertainty in the absolute calibration has four main sources: the measurement of the neutral beam flux ($\pm 18\%$), the estimation of the fraction of $1s_5$ metastable atoms in the fast beam ($\pm 12\%$), the calculation of the beam overlap integral (which includes contributions from both the beam size measurements and the beam positioning) ($\pm 15\%$), and the uncertainty in the ground-state excitation cross section ($\pm 12\%$). When combined with the lesser uncertainties in the measurement of the electron-beam current and the ground-state target density, the total uncertainty in the absolute calibration amounts to $\pm 30\%$.

2. Calibration of other levels

The absolute calibration of the remaining $2p$ cross sections was carried out on the hollow cathode discharge source apparatus using a method described previously [33]. Essentially, the wavelength dependence of the detector efficiency is removed by utilizing the known cross sections for excitation from the ground state [12], and then tying all measurements to the previously determined $1s_5 \rightarrow 2p_9$ excitation cross section. The metastable signal ratios are taken at an electron energy of 10 eV, while the ratio of the ground-state cross sections are performed near the peak of the ground-state cross sections (~ 50 eV),

$$\begin{aligned} Q_{1s_n \rightarrow 2p_x}(10 \text{ eV}) &= Q_{1s_5 \rightarrow 2p_9}(10 \text{ eV}) \left(\frac{n_{1s_5}}{n_{1s_n}} \right) \\ &\times \left[\frac{S_{1s_n \rightarrow 2p_x}(10 \text{ eV})}{S_{1s_5 \rightarrow 2p_9}(10 \text{ eV})} \right] \left[\frac{S_{gs}^{2p_9}(E_{\text{peak}})}{S_{gs}^{2p_x}(E_{\text{peak}})} \right] \\ &\times \left[\frac{Q_{gs}^{2p_x}(E_{\text{peak}})}{Q_{gs}^{2p_9}(E_{\text{peak}})} \right]. \end{aligned} \quad (3)$$

For completeness, we have included in Eq. (3) the ratio of the metastable atom number densities to account for the different number of $1s_5$ and $1s_3$ metastable atoms present in the target. However, in this paper we only report results for excitation out of the $1s_5$ metastable level so this ratio is not needed.

As a cross check of the absolute calibration procedures for the two apparatuses, we also performed the fast-beam absolute calibration for the $2p_6$ and $2p_8$ levels. In both cases, the values agreed to those obtained from the hollow-cathode experiment to better than $\pm 3\%$.

C. Additional corrections

We believe that three additional effects have only a negligible effect on our cross-section measurements: polarization of the fluorescence, excitation from nonmetastable levels, and cascades. We address each of these concerns in the order of potentially increasing importance.

1. Polarization

Alignment of the excited atom's orbitals along a quantization axis, as defined by the electron beam, would introduce both a polarization of the emitted fluorescence and an anisotropy in its emission pattern [23]. This introduces a correction to our measured cross-section values of the form $(1 - P/3)$, where P is the standard definition of optical polarization. Hence, if we entirely ignore polarization, in the worse case scenario of 100% polarization, this introduces only a 33% error in our results. This high level of polarization, however, is rarely found except possibly for electron energies very near the excitation threshold. At high energies (> 15 eV), an expected maximum value of $P = \pm 0.2$ yields only a 7% correction, which is on the order of the statistical uncertainty in the measurements. Our low-energy results (< 15 eV) obtained from the hollow-cathode discharge source should be polarization independent since the optical axis (oriented at 60° to the electron-beam axis) is very close to the magic angle of 54.7° where the emission intensity is equal to the average intensity independent of polarization [23]. We conclude that polarization of the fluorescence produces only a very small change in the optical cross sections and we therefore ignore the effect of polarization.

2. Nonmetastable atoms in target

In addition to the two metastable levels, each atom source also produces a considerable number of atoms in the ground state, and in the two $J=1$ resonant levels of the $2p^5 3s$ configuration. In the case of the hollow-cathode experiment, the overwhelming number of ground-state atoms in the target limits the energy range of the apparatus to energies well below the threshold for excitation from the ground state. The gas pressure *inside* the hollow-cathode discharge is high enough to allow some population buildup of the short lived (~ 20 ns) $2p^5 3s, J=1$ resonant levels by radiation trapping. However, the reduced gas pressure outside the discharge, combined with the $> 15 \mu\text{s}$ flight time of the atoms from the discharge to the collision region severely reduce the contribution from these levels. Clear evidence of this is seen in the

$2p_1$ and $2p_3$ (both $J=0$) excitation functions (see Sec. III A). Both levels have sharply peaked excitation functions characteristic of excitation from nondipole-allowed levels, as compared to the broad energy dependence one would expect for excitation from the $J=1$ resonant levels.

For the fast-beam metastable atom source, the near-resonant charge-exchange process creates about half of the neutral atoms in the $J=1$ levels of the $2p^53s$ configuration. The $7\ \mu\text{s}$ flight time from the charge-exchange cell to the collision region is long enough for these atoms to decay to the ground state. The resulting fast-neutral beam, however, still consists of over 50% ground state atoms. Since this apparatus operates with electron energies above the threshold for ground-state excitation, these atoms are expected to make some small contribution to detected signal. However, the peak ground-state excitation cross section is typically two to three orders of magnitude smaller than the corresponding metastable excitation cross section. Further, the ground-state excitation value falls off much faster with increasing electron energy than does the cross section for excitation from the metastable levels. Thus, the ground-state contribution to our measured signal is less than 1% for all the levels we have measured.

3. Cascades

An excited level is populated both by direct electron-impact excitation and by electron-impact excitation into higher-lying levels followed by spontaneous decay into the excited level of interest. The sum of the direct cross section and the cascade contribution yields the apparent cross section. Chilton *et al.* have shown that for *ground-state* excitation into some levels of the $2p^53p$ configuration, the cascade contribution at some energies can exceed the direct excitation cross section [12]. This pattern is not expected for excitation out of the metastable levels. Excitation into the $2p^53p$ levels correspond to dipole-allowed processes for the metastable levels, which should yield large cross sections. Cascades into the levels of the $2p^53p$ configuration arise mainly from the levels of the $2p^54s$ and $2p^53d$ configurations. Excitation into these levels from the metastable levels should be small due to their dipole-forbidden nature. This is the opposite case from ground-state excitation since excitation from the $2p^6$ ground state into the $2p^53p$ levels correspond to dipole-forbidden processes, whereas excitation from the ground state into some of the levels that cascade into the $2p^53p$ levels are of the dipole-allowed type. In Ref. [12] the cascade transitions were measured with a near-IR Fourier transform spectrometer; unfortunately, the low-signal rates for metastable excitation make direct measurement of the cascading transitions very difficult.

We can, however, use the fast beam apparatus to obtain an upper limit of the cascade contribution using a form of a time-resolved experiment [34]. Due to the high velocity of atoms in the fast beam ($\sim 1.4 \times 10^7\ \text{cm/s}$), atoms travel significant ($\sim \text{mm}$) distances between the point where they are excited by an electron and the point where they decay. By measuring the spatial profile of the fluorescence signal downstream from the electron beam, it is possible to determine the temporal dependence of the excitation signal. Cas-

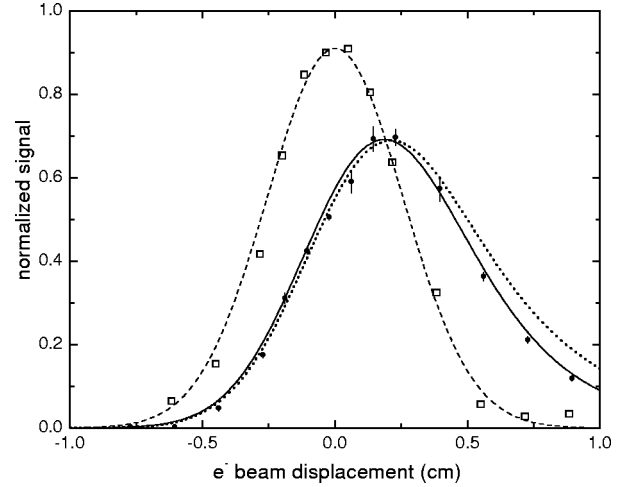


FIG. 2. Cascade analysis of $1s_5 \rightarrow 2p_9$ excitation (at 50 eV) from time resolution provided by use of a fast-beam target. Data points taken with a static gas target (\square) are fitted (dashed line) to find the effective widths of electron beam and optics. The only free parameter used to compare the 1.6-keV Ne^* beam data (\bullet) to the fast-beam modeled calculations is the absolute normalization. Two model calculations are shown: the solid line assumes no cascades, the dotted line assumes a 20% cascade contribution to the signal. See Ref. [34] for details of this method.

cading levels always increase the decay period since the atom must undergo two decays before giving off a detectable photon. Large amounts of cascades would thus inflate the signal measured at long delays/distances after the electron beam pulse/position. Our data for the $1s_5 \rightarrow 2p_9$ excitation process is shown in Fig. 2. A fit to the data indicates that the cascade cross section is $(3 \pm 5)\%$ of the direct cross section for this level. For the $2p_6$ level, the fit yielded a cascade cross section that is only $(10 \pm 7)\%$ of the direct cross section. The actual contribution of cascading levels to our measured signal is less than this amount, since cascading atoms tend to decay downstream of the point where we typically collect fluorescence. This effect further reduces the amount of cascades in the fast-beam “apparent” cross-section measurements by approximately a factor of two [34].

In general we estimate that cascades are less than 5% of the reported apparent cross sections for electron energies over 20 eV. For energies less than 20 eV, the cascades should be less than 10 to 15%, except for excitation into the $J=0$ levels ($2p_1$ and $2p_3$). For these levels, the cascades may be slightly higher since the direct cross section for these levels from the metastable levels is relatively small.

III. RESULTS

A. Mixed target

As mentioned in Sec. II A, the atomic targets used in this paper consist of a mixture of $1s_3$ ($J=0$) and $1s_5$ ($J=2$) metastable atoms. For both sources the $1s_5:1s_3$ ratio of atoms is expected to be 5:1 (statistical weighting). In our previous paper on excitation of metastable argon [33] we used a Ti:Sapphire laser to selectively depopulate one of the two

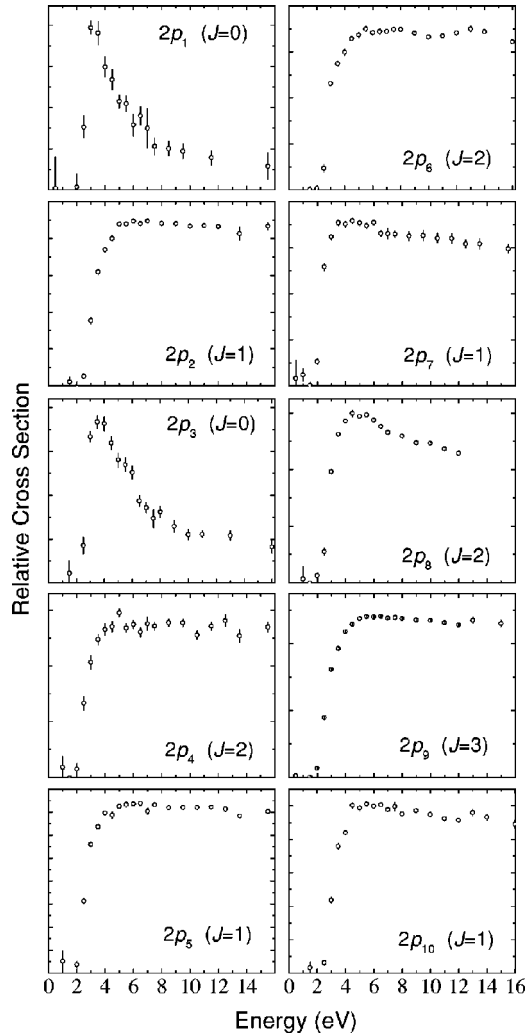


FIG. 3. Relative cross sections for excitation from the mixed target at low energy. Error bars are statistical only.

levels so that we could separately determine the cross section for excitation from each of the two metastable levels. It is relatively common to achieve state selection of a neon metastable beam using dye lasers [35]; however, we have not been able to accomplish this. As a result, the low-energy results presented in this paper are limited to relative results from a mixed target. For excitation into $2p^53p$ levels with $J=2$ and $J=3$, our previous results from metastable argon [33,36] would indicate that the signal should be dominated by excitation from the $1s_5$ ($J=2$) metastable level. These results can then be placed on an absolute scale and are reported in Sec. III B.

The energy dependence of the measured cross sections from the mixed target are shown in Fig. 3. There are two general shapes: a broad maximum for excitation into the $J=1, 2$, and 3 levels, and a sharp peak for excitation into the two $J=0$ levels. The origin of this pattern is illustrated by noting that the interaction between the incident electron and atom is dominated (to first order) by the dipole-interaction term. Excitation into a $J=1, 2$, or 3 level is dipole allowed from one or both of the metastable levels, while excitation into the $J=0$ levels is dipole forbidden from both metastable

levels. This is the same pattern that we observed for excitation of metastable argon [33].

B. Excitation from $1s_5$ level

Excitation into the $J=2$ and 3 levels is dipole allowed from the $J=2$ ($1s_5$) metastable level, but dipole forbidden from the $J=0$ ($1s_3$) metastable level. As a result, we expect that the signal contribution from any $1s_3$ atoms is negligible above 5 eV. At lower energies, the dominance of the dipole-allowed excitation may not be as distinct. Theoretical calculations for Ar indicate that the $1s_3 \rightarrow 2p$ cross section may be the same order of magnitude as the $1s_5 \rightarrow 2p$ cross section below 5 eV [37]. However, since the number density of $1s_3$ atoms is approximately a factor of five less than the number density of $1s_5$ atoms, the contribution to the signal rate should still be less than 10% at low energies.

Since excitation into the four $J=1$ levels is dipole allowed from both metastable levels, in general, we are not able to determine the separate $1s_3 \rightarrow 2p$ and $1s_5 \rightarrow 2p$ cross sections without using a laser to perform state selection on the target. Excitation of the two $J=0$ levels is dipole forbidden from both metastable levels, so it is once again impossible to determine the $1s_5 \rightarrow 2p$ cross section without state selection of the target. Nonetheless, if we assume that all of the signal is due to the $1s_5$ atoms in the target, it is possible to place upper limits on the $1s_5 \rightarrow 2p_1$ and $1s_5 \rightarrow 2p_3$ cross sections. Doing so, we find that the upper limit on the $1s_5 \rightarrow 2p_1$ peak cross sections is $0.40 \times 10^{-16} \text{ cm}^2$, and $0.37 \times 10^{-16} \text{ cm}^2$ for the peak $1s_5 \rightarrow 2p_3$ cross section. Alternatively, if we assume that all of the signal is due to the $1s_3$ atoms in the target, the upper limits on the peak cross sections are both equal to $2 \times 10^{-16} \text{ cm}^2$ for the $1s_3 \rightarrow 2p_1$ and $1s_3 \rightarrow 2p_3$ cross sections.

In Fig. 4, we present excitation functions for the four levels where the signal is dominated by excitation from the $1s_5$ metastable level for incident electron energies up to 450 eV. Values at selected energies are listed in Table II. As discussed in Sec. II C 3, the cascade contribution to the measured apparent cross sections is estimated to be less than 5% at high-electron energies (>40 eV). While a larger contribution at low energies cannot be completely ruled out, we believe the reported numbers are a very good approximation of the direct cross sections.

C. Comparison with experiment and theory

1. Previous experimental work

There have been a number of other experimental measurements related to the measurements reported here [15–20]. Except for the relative excitation function reported by Mityureva and Penkin [15], the other experiments measured rate coefficients in a neon discharge that were inverted into cross-section measurements by using a measured electron temperature and assumed cross-section energy dependence. These discharge results are only sensitive to cross-section values near onset due to the low electron temperature of the discharges. The possible presence of radiation trapped $2p^53sJ=1$ levels further complicates the analysis of these

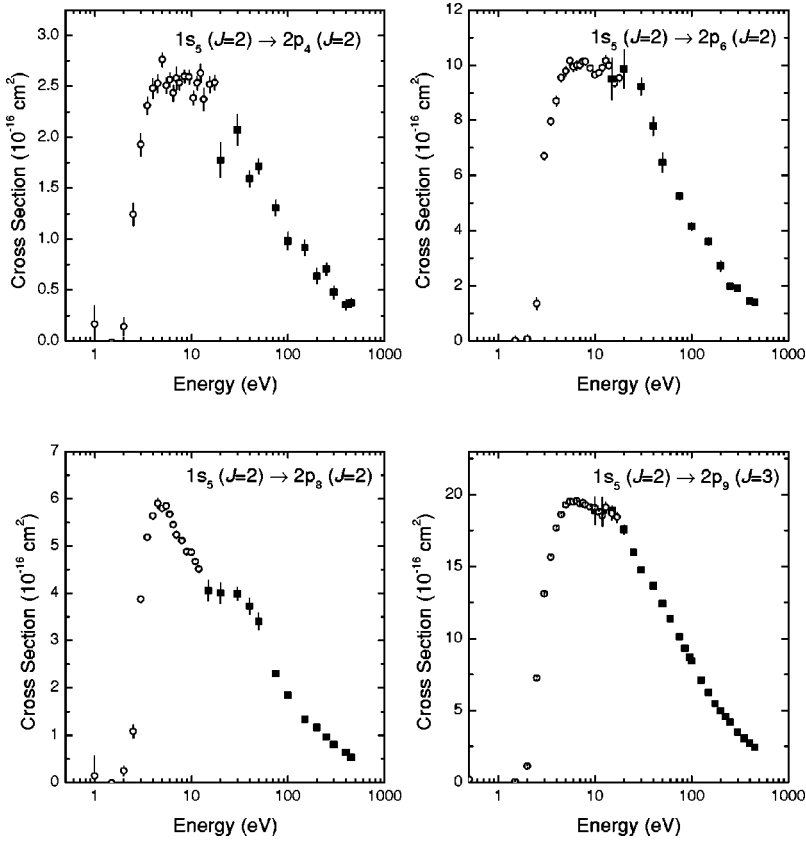


FIG. 4. Absolute cross sections for excitation from the metastable $1s_5$ level. Data points below 15 eV were obtained with the hollow cathode discharge source, points above 15 eV were obtained with the fast-beam target. Error bars are statistical only, and do not include the additional $\pm 30\%$ uncertainty in the absolute calibration.

discharge experiments unless a laser [20] is used to separate out the contribution from each of the four possible initial levels. Thus, quantitative comparisons of the cross sections from these experiments with our measurements must be viewed with care. In the following paragraphs, we discuss briefly each experiment and relate its results with ours.

Behnke *et al.* [19] fitted parameters in a semiempirical formulation of the Born-Bethe approximation to data from a low-pressure glow discharge. For the peak $1s_5 \rightarrow 2p_9$ excitation cross section their fit yields a value of $19 \times 10^{-16} \text{ cm}^2$ that is identical to the value of $(19 \pm 6) \times 10^{-16} \text{ cm}^2$ for our experiment. The agreement for the other three levels, how-

TABLE II. Apparent/direct cross-section results. Units of 10^{-16} cm^2 . Error bars are statistical only and do not include the $\pm 30\%$ uncertainty in the absolute calibration.

Energy (eV)	$Q(1s_5 \rightarrow 2p_4)$ ($J=2$)	$Q(1s_5 \rightarrow 2p_6)$ ($J=2$)	$Q(1s_5 \rightarrow 2p_8)$ ($J=2$)	$Q(1s_5 \rightarrow 2p_9)$ ($J=3$)
2	0.14 ± 0.09	0.06 ± 0.16	0.2 ± 0.1	1.1 ± 0.1
3	1.9 ± 0.1	6.7 ± 0.1	3.9 ± 0.1	13.09 ± 0.04
4	2.5 ± 0.1	8.7 ± 0.2	5.6 ± 0.1	17.7 ± 0.1
6	2.6 ± 0.1	9.9 ± 0.1	5.67 ± 0.05	19.48 ± 0.05
8	2.6 ± 0.1	10.1 ± 0.1	5.11 ± 0.05	19.3 ± 0.1
10	2.5 ± 0.1	9.6 ± 0.1	4.87 ± 0.04	19.1 ± 0.1
15	2.5 ± 0.1	9.6 ± 0.2	4.1 ± 0.2	18.9 ± 0.3
20	1.8 ± 0.2	9.9 ± 0.7	4.0 ± 0.2	17.6 ± 0.3
30	2.1 ± 0.2	9.2 ± 0.3	4.0 ± 0.1	14.8 ± 0.1
50	1.7 ± 0.1	6.5 ± 0.3	3.4 ± 0.2	12.4 ± 0.1
75	1.3 ± 0.1	5.2 ± 0.1	2.3 ± 0.1	10.1 ± 0.1
100	0.98 ± 0.09	4.2 ± 0.1	1.8 ± 0.1	8.43 ± 0.07
150	0.91 ± 0.08	3.6 ± 0.1	1.33 ± 0.06	6.24 ± 0.07
200	0.64 ± 0.08	2.7 ± 0.2	1.16 ± 0.06	4.96 ± 0.05
300	0.48 ± 0.06	1.9 ± 0.1	0.80 ± 0.04	3.51 ± 0.04
400	0.35 ± 0.05	1.4 ± 0.1	0.63 ± 0.03	2.75 ± 0.03

TABLE III. Comparison of $1s_5 \rightarrow 2p_i$ cross-section results. Units of 10^{-16} cm^2 . For the theoretical values and the results of this paper, the values reported are peak cross sections. For other experimental results, the values are mean values weighted over a $\sim 3 \text{ eV}$ electron temperature. Last two columns are the generalized IP-Born values of Hyman combined with optical oscillator calculations of Taylor *et al.* and of Seaton.

Excitation into level	Experiment						Theory		
	This paper	Frish [16]	Beterov [17]	Samson [18]	Behnke [19]	Bortwick [20]	Leveau [38]	Hyman/ Taylor [39,40]	Hyman/ Seaton [39,41]
$2p_4$ ($J=2$)	2.6 ± 0.8		11	7.2	2.0	1.2	3	3.0	3.4
$2p_6$ ($J=2$)	9.8 ± 3.0		22	12	3.1	10	6	11.2	9.4
$2p_8$ ($J=2$)	5.6 ± 1.7		13	20	3.0	6.8	4	6.0	5.8
$2p_9$ ($J=3$)	19 ± 6	12.5	48		19	27	19	27.5	25.5

ever, is not as good. In particular, the value Behnke *et al.* find for the $2p_6$ level is a factor of 3 smaller than our result.

Samson [18] obtained cross sections from optically pumping a neon discharge to determine the excited-state number densities. Since the number density of resonance levels was reported to be an order of magnitude less than the metastable number density, one can equate their measured cross sections into the $J=2$ and 3 levels with the $1s_5 \rightarrow 2p$ excitation cross sections. No values for the $2p_9$ level are reported. The results for the remaining three levels are larger than the present results by a factor of 2.5.

Frish and Revald [16] investigated the role of excitation out of $2p^5 3s$ levels by monitoring the intensity of $2p^5 3p \rightarrow 2p^5 3s$ emission lines as a function of current density in a low-pressure discharge. At the highest discharge currents studied, they state that half of all emissions were due to excitation of $2p^5 3s$ atoms. The composition of the excited state fraction of the target (measured by reabsorption) was found to be 73% $1s_5$, 16% $1s_3$, and 11% $J=1$ resonance levels. They report mean cross sections averaged over the composition of their metastable target. Due to the suspected contribution from the $J=1$ resonance levels to excitation into $2p^5 3p J=1$ and 2 levels, the only level that we can compare directly with is for excitation of the $J=3$ $2p_9$ level. Upon converting their $2p^5 3s \rightarrow 2p_9$ cross section value into a $1s_5 \rightarrow 2p_9$ value, their data yields a value of $13 \times 10^{-16} \text{ cm}^2$, which is a factor of 0.66 smaller than the value reported here, but within error bars.

Beterov and Chebotaev [17] studied excitation out of the metastable levels of neon by placing a glow discharge tube within the cavity of a helium-neon laser. They obtained average excitation rates by monitoring the $2p_4$ to $2s_2$ absorption of the $1.15 \mu\text{m}$ laser line in conjunction with measurements of the fluorescence from the other $2p^5 3p$ levels, and the electron temperature. Then they employed the Born-Bethe approximation to convert these measurements into individual excitation cross sections for each initial state (metastable and resonant levels). On average, the values they report are larger than the present results by a factor of 3.

Bothwick *et al.* [20] have recently reported rate coefficients for excitation out of the $2p^5 3s$ levels using laser collisionally induced fluorescence. Essentially, a laser is used to alter the population of one set of excited states, while the change in fluorescence of another excited state is monitored. This method allows the initial state in the excitation process

to be determined, allowing a much better comparison to our results. The cross sections extracted from their work are in good agreement with those presented here. The largest difference is seen in their $1s_5 \rightarrow 2p_9$ excitation cross section which is 40% larger than the value reported here; while there is excellent agreement on the $1s_5 \rightarrow 2p_6$ excitation cross section.

In contrast to the previously mentioned discharge experiments, Mityureva and Penkin [15] used a monoenergetic electron beam along with a discharge source of metastable atoms to obtain the energy dependence of the $2p_9$ excitation cross section. The composition of the metastable target was not reported. Their relative curve shows a sharp peak, with the cross section decreasing to one tenth the peak value at 10 eV. This is inconsistent with the negligible decrease in cross-section value we observe in the $1s_5 \rightarrow 2p_9$ excitation cross section between 5 and 10 eV. They also report that the largest metastable excitation cross sections are for the $2p_1$ ($J=0$) and $2p_9$ ($J=3$) levels. This is also inconsistent with the small upper limit we found for the $1s_3 \rightarrow 2p_1$ and $1s_5 \rightarrow 2p_1$ excitation cross sections.

2. Comparison to theory

Three sets of theoretical calculations have been published for excitation out of the metastable levels of neon [38–40]. Leevau *et al.* [38] have published peak cross-section values based upon the semiempirical Drawin formula. Their values are in excellent agreement with those we report here with an average difference of only 5%.

Hyman [39] has published results based on the Born approximation, along with modifications based upon Seaton's impact-parameter (IP) theory to extend the results to low energies. These results are based upon average oscillator strengths, and must be combined with sets of optical oscillator strengths to obtain individual excitation cross sections. Table III includes theoretical cross sections obtained by combining Hyman's IP results with the oscillator values from Taylor *et al.* [40] and from Seaton [41] (see, also, Sec. III C 3). For both sets of values there is generally good agreement.

Taylor, Clark, and Fon [40] have calculated excitation cross sections using the *R*-matrix method for energies within 10 eV of threshold. For computational simplicity, neon was treated as an *LS*-coupled atom. Furthermore their calculations did not include separate *J* sublevels for each *LS* state,

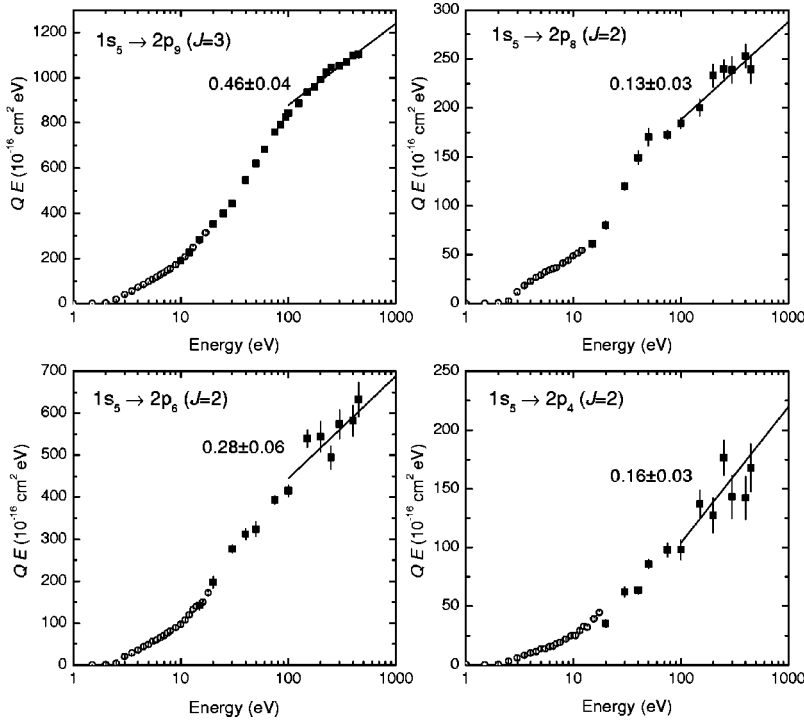


FIG. 5. Born-Bethe plots. Error bars are statistical only. Lines are the linear fits to data above 100 eV used to extract the optical oscillator strength of the corresponding transition.

and therefore can not be compared directly with our data. Nonetheless, of special interest to our work is that their spin-forbidden $2p^5 3s(^3P) \rightarrow 2p^5 3p(^1L)$ excitation cross sections exhibit a sharp peak at electron energies about 1 eV above the excitation threshold. This illustrates the distinction between spin-forbidden excitation and dipole-allowed excitation which has a broad maximum as shown in Fig. 3.

3. Born-Bethe approximation at high energy

In contrast with previous experimental measurements that were only sensitive to cross sections values at low-electron energies where theoretical calculations are generally difficult, the present results extend up high enough in energy to values where the simpler Born-Bethe approximation is expected to be valid. In this high-energy approximation, the excitation cross section for a dipole-allowed transition is given by

$$Q_{ij}(E) = 4\pi a_0^2 f_{ij} \left(\frac{R}{E} \right) \left(\frac{R}{E_{ij}} \right) \ln E + \text{order} \left(\frac{1}{E} \right) + \dots, \quad (4)$$

TABLE IV. Comparison of optical oscillator strengths f_{ik} . Error bars in this paper are for statistical uncertainty in the fit and from the uncertainty in the absolute calibration.

Transition		Experiment			Theory		
	Wavelength (nm)	This paper	Chang and Sester [42]	Inatsugu and Holmes [43]	Wiese <i>et al.</i> [44]	Taylor <i>et al.</i> [40]	Seaton [41]
$1s_5-2p_4$	588.2	$0.16 \pm 0.03 \pm 0.05$	0.0548	0.0601	0.096	0.0506	0.058
$1s_5-2p_6$	614.3	$0.28 \pm 0.06 \pm 0.10$	0.165	0.160	0.122	0.189	0.158
$1s_5-2p_8$	633.4	$0.13 \pm 0.03 \pm 0.04$	0.104	0.0971	0.082	0.101	0.097
$1s_5-2p_9$	640.2	$0.46 \pm 0.04 \pm 0.14$	0.395	0.442	0.373	0.461	0.428

where a_0 is the Bohr radius, R is the Rydberg energy (13.62 eV), E_{ij} is the energy difference between the initial level i and final level j , and f_{ij} is the oscillator strength of the $i \rightarrow j$ optical transition. Hence, at energies high enough to neglect the higher-order terms, a Bethe plot of QE versus $\ln E$ would be linear, with a slope proportional to the oscillator strength of the corresponding optical transition.

In Fig. 5, we show Bethe plots of our cross-section results. In Table IV, we list oscillator strengths extracted from linear fits to the data in Fig. 5. In this process, we have arbitrarily set the lower bound of the data included in the fit to be 100 eV. For the case of $1s_5 \rightarrow 2p_9$, where the statistical noise is smallest, there are indications that the slope is not constant until at least 300 eV. However, it is difficult to extract a robust estimate of the slope using only values above 300 eV due to the limited number of measurements we have above this energy. This decrease in the slope is less evident in the Bethe plots of the other four levels. If this decrease in the slope is a real effect, it may explain why our extracted oscillator strengths are generally larger than the other experimental [42,43] and theoretical [40,41,44] values listed in Table IV.

IV. DISCUSSION

The patterns observed in the excitation of metastable neon are in general accordance with our earlier works on the excitation of metastable helium [24,32,45] and metastable argon [33]. Since neon is intermediate between the strongly LS coupled case of helium, and the intermediate coupling of argon, it is interesting to point out a few of the similarities and differences observed between the three atoms.

In all three atoms, we have observed excitation out of a metastable level [$1s2s(2^3S)$ for He, $2p^53s(3P_2)$ for Ne, and $3p^54s(3P_{0,2})$ for Ar], into level(s) in the next higher configuration ($1s2p$ for He, $2p^53p$ for Ne, and $3p^54p$ for Ar) which is also optically connected to the initial configuration. Excitation of this type is generally most favorable on account of the optically allowed nature of the excitation and the small excitation energy. Indeed, the peak neon $1s_5 \rightarrow 2p_9$ metastable excitation cross section is over 3000 times the peak $2p^6(^1S_0) \rightarrow 2p_9$ ground-state excitation cross section. The corresponding metastable to ground state $2p_9$ excitation ratio is over 470 for argon [33]. Likewise, in the case of He, the ratio of cross sections for excitation into the 2^3P level from the 2^3S metastable level versus from the 1^1S ground level is over 5000 [32].

One interesting pattern seen in the three atoms is the energy at which the cross section enters the “Born-regime.” For optically allowed excitations out of a metastable level such as He($2^3S \rightarrow 3^3P$), Ne($1s_5 \rightarrow 2p_9$), and Ar($1s_5 \rightarrow 2p_9$), Bethe plots yielded oscillator strength in agreement with accepted spectroscopic values for energies above 50 eV for He [24] and Ar [33], whereas in the present case of Ne, the Born-regime occurs at somewhat higher energies (≥ 200 eV). In contrast, our measurements of optically forbidden-type excitations out of the He(2^3S) metastable level into the 3^3S , 3^3D , and 4^3D levels did not conform to “Born-like” behavior at energies as high as 1000 eV [24]. This drastic difference in the Born-Bethe threshold between optically allowed and optically forbidden excitations is seen only in the excitation out of metastable levels but not in the excitation out of the ground level. The reason for this is not understood at the present time.

Neon and argon present an additional dimension in the excitation process over helium because the final configurations of Ne and Ar ($2p^53p$ and $3p^54p$, respectively) contain ten energy levels (labeled $2p_1$ to $2p_{10}$ in Paschen’s notation for both atoms) where the cross sections vary significantly from one level to another. For example, in our paper on argon we found the ratio of the peak cross sections for metastable excitation to ground-state excitation to vary between 730 (for $2p_4$) and 10 (for $2p_1$) [33]. Recalling that the threshold for excitation into the $2p$ levels from the meta-

stable levels is only ~ 2 eV, which is much smaller than the excitation threshold from the ground level (13 eV for Ar, 18 eV for Ne), the large variation of the cross-section ratio cited above suggest interesting applications to the diagnostics of ionized gases [3,4]. Consider a plasma containing a trace of Ar atoms. Some levels, for example, the $2p_4$ ($J=1$), $2p_6$ ($J=2$), and $2p_9$ ($J=3$) levels, will be primarily populated by electron-impact excitation of metastable atoms because of their large cross sections and because of the much larger abundance of “slow” electrons (~ 2 eV) over the fast electrons (13 eV), even though the metastable-atom concentration may be as low as 1 part in 10^5 of the ground-state atoms. On the other hand, the $2p_1$ ($J=0$) level is excited primarily from the ground level because for this level, the metastable to ground-state excitation cross-section ratio is only about ten, not enough to offset the small metastable concentration. Thus, emissions from the $2p_9$ and $2p_1$ levels can be used to monitor the distribution of the “slow” and “fast” electrons.

In the absence of the laser-assisted state selection of the metastable target, the present paper on neon is not as comprehensive as our earlier efforts on metastable argon. Nonetheless, our neon results reflect similar trends to argon. For example, as in argon the peak excitation cross sections into the $J=2$ levels ($2p_4, 2p_6, 2p_8$) and into the $J=3$ ($2p_9$) level from the $1s_5$ level, which correspond to electric-dipole transitions, are large ranging from 2.6×10^{-16} to 19×10^{-16} cm². For the optically forbidden excitations from the $1s_5$ to the $J=0$ levels ($2p_1$ and $2p_3$), we have obtained an upper limit of the peak excitation cross section of 0.40×10^{-16} cm² for the $1s_5 \rightarrow 2p_1$ excitation and 0.37×10^{-16} cm² for the $1s_5 \rightarrow 2p_3$ excitation. These upper limits are much smaller than the excitation cross sections into the optically allowed levels. Moreover, the energy dependence of the excitation cross sections into the $J=0$ levels are very different from the excitation shapes out of the $1s_5$ level to the $J=2$ and $J=3$ levels. Thus, as in the case of argon, fluorescence from the various $2p$ emission lines of the neon atom may serve as a useful diagnostic tool for determining electron temperatures and spatial distributions of metastable atoms in ionized gas systems. The cross sections obtained in this paper will also provide a benchmark similar to our earlier argon results for the testing of theoretical calculations [37,46,47].

ACKNOWLEDGMENTS

The authors wish to thank Dan Sullivan, Karl Jablonowski, and Zak Staniszewski for their assistance in some of the measurements. This work was supported by the National Science Foundation and Air Force Office of Scientific Research.

- [1] T. Bräuer, S. Gortchakov, D. Loffhagen, S. Pfau, and R. Winkler, J. Phys. D **30**, 3223 (1997).
- [2] J. H. Jacobs and J. A. Mangano, Appl. Phys. Lett. **28**, 724 (1976).

- [3] M. V. Malyshev and V. M. Donnelly, Phys. Rev. E **60**, 6016 (1999).
- [4] S. A. Moshkalyov, P. G. Steen, S. Gomez, and W. G. Graham, Appl. Phys. Lett. **75**, 328 (1999).

- [5] W. L. Nighan, IEEE Trans. Electron Devices **28**, 625 (1981).
- [6] A. Javan, Phys. Rev. Lett. **3**, 87 (1959).
- [7] N. D. Bhaskar and A. Lurio, Phys. Rev. A **13**, 1484 (1976).
- [8] R. S. Van Dyck, Jr., C. E. Johnson, and H. A. Shugart, Phys. Rev. A **5**, 991 (1972).
- [9] M. H. Phillips, L. W. Anderson, and C. C. Lin, Phys. Rev. A **32**, 2117 (1985).
- [10] S. Tsurubuchi, K. Arakawa, S. Kinokuni, and K. Motohashi, J. Phys. B **33**, 3713 (2000).
- [11] A. A. Mityureva and V. V. Smirnov, J. Phys. B **27**, 1869 (1994).
- [12] J. E. Chilton, M. D. Stewart, Jr., and C. C. Lin, Phys. Rev. A **61**, 052708 (2000).
- [13] F. A. Sharpton, R. M. St John, C. C. Lin, and F. E. Fajen, Phys. Rev. A **2**, 1305 (1970).
- [14] I. P. Bogdanova and S. V. Yurgenson, Opt. Spektrosk. **63**, 1373 (1987) [Opt. Spectrosc. **63**, 815 (1987)].
- [15] A. A. Mityureva and N. P. Penkin, Opt. Spektrosk. **38**, 404 (1975) [Opt. Spectrosc. **38**, 229 (1975)].
- [16] S. E. Frish and V. F. Revald, Opt. Spektrosk. **15**, 726 (1963) [Opt. Spectrosc. **15**, 395 (1963)].
- [17] I. M. Beterov and V. P. Chebotaev, Opt. Spektrosk. **23**, 854 (1967) [Opt. Spectrosc. **23**, 467 (1967)].
- [18] A. V. Samson, Opt. Spektrosk. **42**, 570 (1977) [Opt. Spectrosc. **42**, 321 (1977)].
- [19] J. F. Behnke, H. Deutsch, and H. Scheibner, Contrib. Plasma Phys. **25**, 41 (1985).
- [20] I. S. Bothwick, A. M. Paterson, D. J. Smith, and R. S. Stewart, J. Phys. B **33**, 4513 (2000).
- [21] M. Johnston, K. Fujii, J. Nickel, and S. Trajmar, J. Phys. B **29**, 531 (1996).
- [22] A. J. Dixon, M. F. A. Harrison, and A. C. H. Smith, in *Proceedings of the Eighth International Conference on the Physics of Electronic and Atomic Collisions*, edited by B. C. Corbic and M. V. Kurepa (Institute of Physics, Belgrade, 1973), Vol. 1.
- [23] A. R. Filippelli, C. C. Lin, L. W. Anderson, and J. W. McCorkney, Adv. At., Mol., Opt. Phys. **33**, 1 (1994).
- [24] J. B. Boffard, M. E. Lagus, L. W. Anderson, and C. C. Lin, Phys. Rev. A **59**, 4079 (1999).
- [25] J. B. Boffard, M. E. Lagus, L. W. Anderson, and C. C. Lin, Rev. Sci. Instrum. **67**, 2738 (1996).
- [26] G. A. Piech, M. E. Lagus, L. W. Anderson, C. C. Lin, and M. R. Flannery, Phys. Rev. A **55**, 2842 (1997).
- [27] R. B. Lockwood, L. W. Anderson, and C. C. Lin, Z. Phys. D: At., Mol. Clusters **24**, 155 (1992).
- [28] R. H. Neynaber and G. D. Magnuson, J. Chem. Phys. **65**, 5239 (1976).
- [29] M. J. Coggiola, T. D. Gaily, K. T. Gillen, and J. R. Peterson, J. Chem. Phys. **70**, 2576 (1979).
- [30] F. W. Meyer and L. W. Anderson, Phys. Rev. A **9**, 1909 (1974).
- [31] A. Viehl, M. Kanyo, A. Van der Hart, and J. Schelten, Rev. Sci. Instrum. **64**, 732 (1993).
- [32] G. A. Piech, J. E. Chilton, L. W. Anderson, and C. C. Lin, J. Phys. B **31**, 859 (1998).
- [33] J. B. Boffard, G. A. Piech, M. F. Gehrke, L. W. Anderson, and C. C. Lin, Phys. Rev. A **59**, 2749 (1999).
- [34] J. B. Boffard, M. F. Gehrke, M. E. Lagus, L. W. Anderson, and C. C. Lin, Eur. Phys. J. D **8**, 193 (2000).
- [35] See for example, F. B. Dunning, T. B. Cook, W. P. West, and R. F. Stebbing, Rev. Sci. Instrum. **46**, 1072 (1975); J. A. Brand, J. E. Furst, T. J. Gay, and L. D. Schearer, *ibid.* **63**, 163 (1992); T. D. Gaily, M. J. Coggiola, J. R. Peterson, and K. T. Gillen, *ibid.* **51**, 1168 (1980).
- [36] G. A. Piech, J. B. Boffard, M. F. Gehrke, L. W. Anderson, and C. C. Lin, Phys. Rev. Lett. **81**, 309 (1998).
- [37] K. Bartschat and V. Zeman, Phys. Rev. A **59**, R2552 (1999).
- [38] J. Leveau, S. Valignat, and F. Deigat, J. Phys. (France) **38**, L385 (1977).
- [39] H. A. Hyman, Phys. Rev. A **24**, 1094 (1981).
- [40] K. T. Taylor, C. W. Clark, and W. C. Fon, J. Phys. B **18**, 2967 (1985).
- [41] M. J. Seaton, J. Phys. B **31**, 5315 (1998).
- [42] R. S. F. Chang and D. W. Setser, J. Chem. Phys. **72**, 4099 (1980).
- [43] S. Inatsugu and J. R. Holmes, Phys. Rev. A **8**, 1678 (1973).
- [44] W. L. Wiese, M. W. Smith, and B. M. Glennon, *Atomic Transition Probabilities*, Natl. Bur. Stand. (U.S.) Circ. No. NSRDS-NBS 4 (U.S. GPO, Washington, DC, 1966), Vol. I.
- [45] M. E. Lagus, J. B. Boffard, L. W. Anderson, and C. C. Lin, Phys. Rev. A **53**, 1505 (1996).
- [46] C. M. Maloney, J. L. Peacher, K. Bartschat, and D. H. Madison, Phys. Rev. A **61**, 022701 (2000).
- [47] A. Dasgupta, M. Blaha, and J. L. Giuliani, Phys. Rev. A **61**, 012703 (2000).